Classification of Error Correcting Codes and Estimation of Interleaver Parameters in a Noisy Transmission Environment

Swaminathan R and A. S. Madhukumar, *Senior member, IEEE*

***Abstract*—Channel encoder, which includes a forward error correcting (FEC) code followed by an interleaver, plays a vital role in improving the error performance of digital storage and communication systems. In most of the applications, the FEC code and interleaver parameters are known at the receiver to decode and de-interleave the information bits, respectively. But the blind/semi-blind estimation of code and interleaver parameters at the receiver will provide additional advantages in applications such as adaptive modulation and coding, cognitive radio, non-cooperative systems, etc. The algorithms for the blind estimation of code parameters at the receiver had previously been proposed and investigated for known FEC codes. In this paper, we propose algorithms for the joint recognition of the type of FEC codes and interleaver parameters without knowing any information about the channel encoder. The proposed algorithm classify the incoming data symbols among block coded, convolutional coded, and uncoded symbols. Further, we suggest analytical and histogram approaches for setting the threshold value to perform code classification and parameter estimation. It is observed from the simulation results that the code classification and interleaver parameter estimation are performed successfully over erroneous channel conditions. The proposed histogram approach is more robust against the analytical approach for noisy transmission environment and system latency is one of the important challenges for the histogram approach to achieve better performance.**

***Index Terms*—Adaptive modulation and coding, blind/semi-blind estimation, block interleaver, cognitive radio, forward error correcting (FEC) code.**

I. Introduction

The random errors introduced by the noisy channel are detected or corrected with the help of forward error correcting (FEC) codes by introducing redundant bits, which in turn reduces the spectral efficiency. Therefore, devising new error correcting/controlling codes without sacrificing the spectral efficiency to a greater extent is always under development. In general, there are two major classes of FEC codes: 1) Block Codes and 2) Convolutional codes. Further, the effect of burst errors due to noisy channel can be minimized with the help of interleavers by rearranging the bit positions of the data stream before transmission. There are different types of interleavers such as block interleavers, which include matrix and helical scan interleavers, convolutional interleaver, helical interleaver, etc. proposed in the literature.

Swaminathan R & A. S. Madhukumar are with the School of Computer Science and Engineering, Nanyang Technological University, Singapore-639798, (e-mail: sramabadran@ntu.edu.sg, asmadhukumar@ntu.edu.sg).

Since block interleavers are more prominently used in error control systems, our discussions are prominently restricted to the same. A block interleaver receives a block of symbols, rearranges them without removing any of the symbols. In particular, a matrix-based block interleaver stores each block of data symbols row-wise in an interleaver matrix and sends column-wise for transmission such that the neighboring data symbols encounter independent fading. The interleaver size or period for matrix-based block interleaver is given by $\beta = N_r \times N_c$, where N_r and N_c denote the number of rows and columns of the interleaver matrix, respectively and an example for interleaver operation is shown in Fig. 1.

In the case of digital video and audio broadcasting systems, interleaving at FEC encoder output is included to improve the performance over a burst error scenario [1]. In most of the broadcast applications, the type of FEC codes, code and interleaver parameters are known at the receiver. With the evolution of modern digital communication systems, designing separate receiver decoding system for every broadcast applications is a costly and a tedious process. Hence, there is a need to design an intelligent broadcast receiver system which adapts itself to any specific broadcast applications. It is also mandatory for the intelligent or cognitive-radio-based broadcast receiver system to blindly estimate the code and interleaver parameters in order to adapt to the variations in the channel coding schemes for extracting the original data [2]. Adaptive modulation and coding (AMC) techniques are also being extensively used in digital video broadcasting (DVB) systems. In the case of AMC-based systems, control channel will signal the modulation and code parameters to the receiver. Hence, the blind recognition of code parameters will lead to conservation of channel resources in the AMC-based broadcast systems. For example, the popular DVB-satellite-second generation (DVB-S2) systems use AMC techniques [3] and in [4], a novel AMC framework has been proposed for DVB-handheld (DVB-H) systems.

Wireless sensor networks (WSNs) also adopt the AMC framework as indicated in [5]. In this case, the blind estimation techniques will reduce the energy consumption in the wireless sensor nodes, as the nodes need not frequently transmit the overheads to specify changes in the code and modulation parameters. Data transmission rate of sensor nodes can also be improved if overheads are not transmitted. Apart from broadcast and wireless sensor network applications, the blind estimation techniques are also beneficial in non-cooperative systems as mentioned in [6] and [7]. This is because, non-

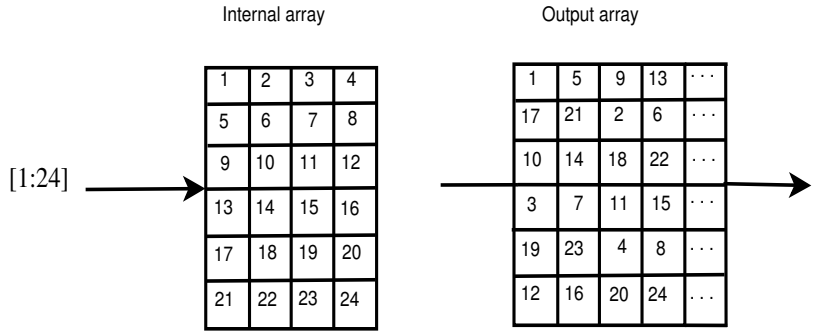

Fig. 1. Matrix block interleaver operation assuming $N_r = 6$ and $N_c = 4$ considering input values $[1 : 24]$

cooperative-based military and spectrum surveillance systems may not have full knowledge about the code and interleaver parameters used in the transmitter. Hence, there is a need for the blind estimation techniques to decode and de-interleave the message bits. It is also useful in the study of DNA sequences to identify possible error correcting codes in the genetic code as mentioned in [8] and [9]. Similarly, the blind estimation strategies will provide a lot of flexibility in designing the receiver decoding system for satellite communication and digital storage systems, since error correcting codes and interleavers are extensively used in these two applications.

The code parameter estimation techniques were investigated extensively in the literature assuming the type of FEC codes is known at the receiving end. In [2], [10], and [11], the parameter estimation of convolutional codes was investigated based on the dual code method. Some interesting dual code properties for the blind recognition of convolutional encoder were proposed in [12]. The blind recognition of convolutional code parameters was restricted to Galois field GF(2) in [2] and [10]-[12]. However, in [13], the parameter estimation of convolutional codes was extended to GF(2^m) case considering noiseless environment. In [14] and [15], the parameter estimation of binary cyclic codes was carried out with a prior knowledge on the type of FEC codes. Furthermore, in [16], two new algorithms for recognizing the parameters of generic and punctured convolutional codes in the presence of bit errors were proposed and they require only few thousand bits to identify the parameters. In [17], an algebraic method for semi-blind recovery of puncturing pattern and punctured code parameters from erroneous bit stream was proposed considering convolutionally encoded data. Firstly, the algorithm was proposed for rate $1/n$ convolutional codes and the same was extended further to rate k/n codes, where k denotes the code dimension and n denotes the codeword length. In [18], the blind identification of the codeword length for various non-binary error correcting codes has been extensively studied over noisy environment. Novel code parameter recognition of binary low-density parity-check (LDPC) codes and convolutional codes was investigated in [19] and [20], respectively, and the proposed method was based on the computation of average log-likelihood ratios (LLRs) of the syndrome a posteriori probability. Instead of average LLR, the blind recognition of rate 1/2 convolutional codes was proposed in [21] using average likelihood difference of the parity checks. Finally, in [22] and [23], the parameter estimation of turbo codes was carried out using iterative expectation-maximization (EM) and least square methods, respectively.

Algorithms for the parameter estimation of block interleaver were proposed and analyzed in [6] and [24] considering a noisy or erroneous transmission environment. The proposed methodology converts a received data matrix into a lower triangular matrix using Gauss-Jordan elimination through pivoting (GJETP) [25]. Further, the algorithm estimates the interleaver size or period from the lower triangular matrix. The proposed methodologies in [6] and [24] were valid only for binary coded data. In [26], the interleaver size estimation algorithm was extended to non-binary coded data. Similarly, the algorithms for estimating convolutional interleaver parameters were proposed in [27] and [28]. Finally, code classification techniques over non-erroneous scenario were studied in [29]. Therefore, to the extent of our knowledge, the joint detection of block interleaver parameters and the type of FEC codes has not been investigated in the literature.

A. **Motivations**

The main motivations behind the proposed work are as follows:

- Though block interleaver parameter estimation algorithm was proposed in [6], [24], and [26], it was restricted only for the case when interleaver period β is a multiple of n. Moreover, the type of FEC codes was also assumed to be known at the receiver, as the interleaver parameter estimation techniques were carried out considering block coded data.
- In addition, only size of the block interleaver matrix (i.e. $N_r \times N_c$) was estimated in [6], [24], and [26]. However, N_r and N_c should also be estimated to successfully de-interleave the message symbols.
- The code classification algorithms to classify the incoming coded data symbols among block coded, convolutionally coded, and uncoded symbols considering erroneous scenario had not been investigated rigorously in the previous works. In [29], the code classification techniques were studied only for non-erroneous scenario.
- It is also to be noted that the LLR-based technique proposed in [19] and [20] for the identification of FEC encoder was not strictly blind. This is because, a prede-

fined set of encoders was assumed to be known at the transmitter and receiver.

B. Contributions

The main contributions of our work are as follows:

- A generalized framework for code classification and block interleaver parameter estimation is proposed.
- Different types of FEC codes exhibit different characteristics owing to their structural differences. Thus, novel methodologies are developed to identify the characteristic variances in order to classify the incoming FEC coded data symbols among block coded, convolutionally coded, and uncoded with or without the presence of interleavers.
- Unlike the prior works, interleaver period β is estimated using the proposed methodology without restricting the same as a multiple of n.
- Apart from estimating β, an algorithm for recognizing N_r and N_c has also been proposed to de-interleave the message symbols successfully.
- Finally, the proposed algorithms are extensively simulated considering a noisy transmission environment and the limitations of the algorithms are also discussed.

The rest of the paper is organized as follows. In section II, a generic block diagram explaining the process of code classification and interleaver parameter estimation is shown. The steps for the joint recognition of the type of error correcting codes and interleaver period are given in Section III and IV for error-free and erroneous scenarios, respectively. In addition, different methodologies for fixing optimal threshold values are also discussed in Section IV. In Section V, the algorithm to estimate N_r and N_c is proposed. Further, the simulation results validating the proposed claims are reported in Section VI. Finally, the concluding remarks are given in Section VII.

II. Parameter Estimation process

The block diagram illustrating the joint detection of the type of FEC codes and interleaver parameters is given in Fig. 2. After receiving the erroneous synchronized data symbols, firstly, the joint recognition of the type of error correcting codes and β is carried out. Secondly, from β, rest of the interleaver parameters i.e. N_r and N_c are estimated and the process is followed by the actual de-interleaving. Finally, the code parameters of the corresponding FEC codes are recognized. Since the code parameter estimation algorithms have been rigorously investigated in the prior works, in this paper, our discussions are restricted to code classification and estimation of interleaver parameters. Similarly, for the case without interleaver, the block diagram can be modified accordingly by removing the interleaver and de-interleaver blocks.

III. Code classification and interleaver period estimation over non-erroneous scenario

The steps for code classification and estimation of interleaver period over non-erroneous scenario are given below.

- Step 1: Reshape the interleaved data symbols into a matrix S, referred as data matrix, of size $a \times b$, where a and b indicate the number of rows and columns of S, respectively.
- Step 2: Assume $a \geq k_1.b$ for simplicity without loss of generality, where k_1 is a constant. It is to be noted that higher the value of k_1, better is the accuracy.
- Step 3: Convert the data matrix S into a column echelon form F using modified GJETP algorithm[1] [25] as follows

$$S.\chi = F\,, \tag{1}$$

where χ denotes the column permutation matrix.
- Step 4: Evaluate the rank $\rho(S)$ by calculating the number of non-zero columns in F and the rank ratio p is given by $p = \rho(S)/b$. Calculate $\rho(S)$ by varying b.
- Step 5: Observe the difference between the successive number of columns with rank deficiency. The difference gives β or lcm(n, β) for the case with interleaver. For the case without interleaver, the difference gives n.

Proposition 1: With block interleaver

Let S be an interleaved data matrix of coded symbols with b columns, β be the interleaver period, and n be the codeword length. If $b = \alpha.\beta$ and $\beta = \gamma.n$, where α and γ are positive integers, then the rank of S, $\rho(S)$ is given by

$$\rho(S) = \alpha.\gamma.k + m \; < \; b \tag{2}$$

and

$$\rho(S) = \alpha.\gamma.k < b \tag{3}$$

for rate k/n convolutional and block codes, respectively.

Proof:

Convolutional codes: It is to be noted that n output convolutionally coded data symbols depend on k present and m previous input uncoded data symbols as mentioned in [2] and [11], where m denotes the memory of convolutional encoder. Similarly, $\alpha.n$ output coded data symbols depend on $\alpha.k$ present and m previous input uncoded symbols (i.e. $\alpha.k + m$ symbols). Therefore, if the convolutionally coded data is block interleaved and if $b = \alpha.\beta$ with $\beta = \gamma.n$, then $\alpha.\gamma$ codewords in a particular row will depend on $\alpha.\gamma.k + m$ symbols and the same is also applicable to all other rows of S. Moreover, the message and parity bits of $\alpha.\gamma$ codewords in all the rows will be properly aligned in the same column. Therefore, after converting S into F through modified GJETP algorithm assuming $b = \alpha.\gamma.n$, there will be only $\alpha.\gamma.k + m$ non-zero or independent columns out of b columns and thus, the deficient rank value $\rho(S)$ is given by (2). The reason for rank deficiency in the case of convolutional codes has also been explained in Appendix A with the help of a case study. Moreover, the inequality $\alpha.\gamma.k + m < b$ holds true or the rank deficiency can be obtained only when $\alpha \geq \alpha_{\text{min}}$ or $b \geq b_{\text{min}}$. The expressions for α_{min} and b_{min} are derived as follows:

[1]Since row permutation is not included to convert S into F, it has been termed as modified GJETP

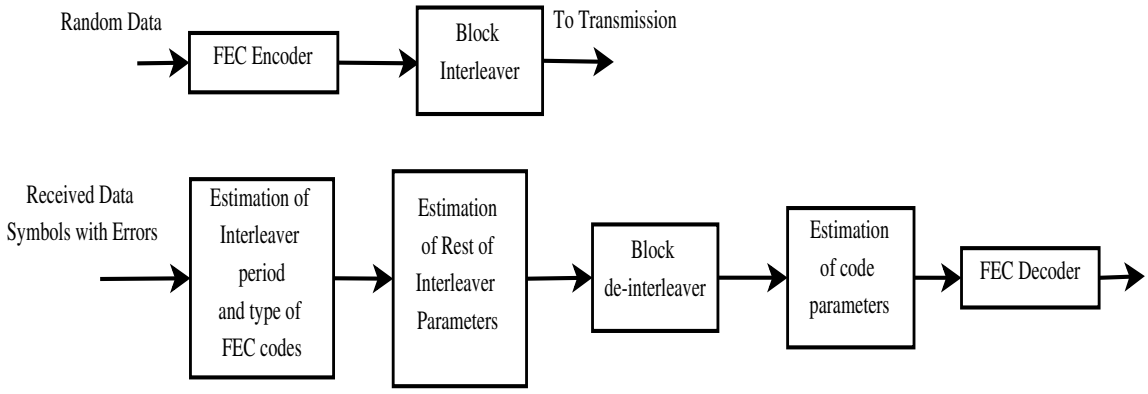

Fig. 2. Generic block diagram for code classification and interleaver parameter estimation process considering block interleaver

After substituting $b=\alpha.\gamma.n$, (2) can be written as

$$\alpha.\gamma.k+m<\alpha.\gamma.n \tag{4}$$

After rearranging, (4) can be written as

$$\alpha.\gamma.n.\left(1-\frac{k}{n}\right)>m\,, \tag{5}$$

$$\alpha.\gamma.n>\frac{n}{n-k}m\,, \tag{6}$$

$$\alpha>\frac{m}{\gamma.(n-k)}\,. \tag{7}$$

Now the minimum value of α, denoted by α_{min}, is given by

$$\alpha_{\text{min}}=\left\lfloor\frac{m}{\gamma.(n-k)}\right\rfloor+1\,, \tag{8}$$

where $\lfloor x\rfloor$ indicates floor(x). From (8), b_{min} is given by

$$b_{\text{min}}=\left(\left\lfloor\frac{m}{\gamma.(n-k)}\right\rfloor+1\right).\beta \tag{9}$$

Block codes: For block codes, it is to be noted that n output coded data symbols depend only on k input uncoded data symbols unlike convolutional codes, since $m=0$. Therefore, the deficient rank $\rho(S)$ is given by (3). The inequality $\alpha.\gamma.k<b$, where $b=\alpha.\gamma.n$, remains true irrespective of α, since $k<n$. Hence, $\alpha_{\text{min}}=1$ and $b_{\text{min}}=\beta$ for block codes. Further, the explanation regarding the reason for rank deficiency remains same as that of convolutional codes.

Corollary 1:

If $\beta\neq\gamma.n$, then the rank deficiency will be obtained for the case when $b=\alpha.\text{lcm}(n,\beta)$, where $\text{lcm}(n,\beta)=\gamma.n$. However, if $b\neq\alpha.\beta$ or $b\neq\alpha.\text{lcm}(n,\beta)$ (i.e. $b\neq\alpha.\gamma.n$), then $\rho(S)=b$, the full rank of the data matrix. In such cases, the message and parity bits of $\alpha.\gamma$ codewords in all the rows will not be properly aligned in the same column, which will lead to the detection of full rank.

Estimation of r and β:

The rank ratio p is given by

$$p=\frac{\rho(S)}{b} \tag{10}$$

Substituting $b=\alpha.\beta$ in (10), where $\beta=\gamma.n$, the rank ratio p for convolutional codes is given by

$$p=r+\lambda\,, \tag{11}$$

where $r=\frac{k}{n}$ and $\lambda=\frac{m}{b}$. Similarly, for block codes after substituting $b=\alpha.\beta$ in (3), p is given by

$$p=r\,. \tag{12}$$

From proposition 1, β (i.e. for the case when β is a multiple of n) or $\text{lcm}(n,\beta)$ (i.e. for the case when β is not a multiple of n) for both convolutional and block codes can be identified by observing the difference between the successive number of columns with rank deficiency. Let $b=\alpha.\gamma.n$ and $b'=(\alpha+1).\gamma.n$ indicate the two rank deficient columns and their difference is given by

$$\begin{aligned} b'-b &= (\alpha+1).\gamma.n-\alpha.\gamma.n \\ &= \gamma.n \\ &= \beta \text{ or } \text{lcm}(n,\beta) \end{aligned} \tag{13}$$

The difference between two successive rank deficient values $\rho(S)$ and $\rho'(S)$ corresponding to b and b', respectively, is given by

$$\begin{aligned} \rho'(S)-\rho(S) &= ((\alpha+1).\gamma.k+m)-(\alpha.\gamma.k+m) \\ &= \gamma.k \end{aligned} \tag{14}$$

By dividing (14) with (13), the code rate r can be estimated as follows:

$$\frac{\rho'(S)-\rho(S)}{b'-b}=r \tag{15}$$

For block codes, the above steps are applicable for estimating r by assuming $m=0$. Hence, r can be estimated from (15) for both convolutional and block codes.

TABLE I
MINIMUM NUMBER OF COLUMNS REQUIRED TO OBTAIN THE FIRST RANK DEFICIENT MATRIX FOR DIFFERENT CONVOLUTIONAL CODES

No.	Code rate (r)	n	k	Y	$b_{\min}$	g_i^j
1	1/2	2	1	3	6	[5,7]
2				4	8	[15,17]
3				5	10	[23,35]
4				6	12	[65,57]
5				6	12	[75,53]
6				7	14	[133,171]
7				8	16	[345,237]
8				9	18	[561,753]
9				10	20	[1167,1545]
10				11	22	[2335,3661]
11	1/3	3	1	4	6	[13,15,17]
12				7	12	[133,165,171]
13				10	15	[1117,1365,1633]
14	1/4	4	1	7	12	[133,171,117,165]

Proposition 2: Without block interleaver

Let S be a data matrix of coded symbols with b columns. If $b = \alpha.n$, then $\rho(S)$ for convolutional and block codes are, respectively, given by

$$\rho(S) = \alpha.k + m < b\,. \tag{16}$$

and

$$\rho(S) = \alpha.k < b\,. \tag{17}$$

Proof:

Convolutional codes: Considering convolutional codes, if $b = \alpha.n$, then α codewords of size equal to $\alpha.n$ bits in a particular row will be a linear combination of $\alpha.k + m$ input bits and the same is applicable to all the other rows. Since the message and parity bits of α codewords in all the rows will be aligned properly in the same column for the case when $b = \alpha.n$, there will be only $\alpha.k + m$ non-zero or independent columns out of b columns after converting S into F. Thus, the deficient rank value $\rho(S)$ is given by (16). Similar to proposition 1, the inequality $\alpha.k + m < b$ given by (16) holds true or the rank deficiency can be obtained only when $\alpha \geq \alpha_{\min}$ or $b \geq b_{\min}$. The expressions for $\alpha_{\min}$ and $b_{\min}$ considering the case without interleaver can be obtained from (8) and (9) by substituting $\gamma = 1$. Based on the given expression, we have also tabulated the minimum number of columns $b_{\min}$ required to obtain the first rank deficient matrix in Table I considering convolutional codes with different r and constraint length Y values. Note that $m = Y - 1$ for rate $1/n$ convolutional codes [30]. It has been observed from the tabulated values that there exist a one-to-one correspondence between $b_{\min}$ and Y for a particular rate r.

Block codes: For block codes, the explanation remains same as that of convolutional codes except for the fact that no memory is involved (i.e. $m = 0$). In Appendix B, another case study explaining the reason for rank deficiency in the case of block codes without interleaver is given.

Corollary 2:

If $b \neq \alpha.n$, then $\rho(S) = b$, the full rank of the data matrix. In such cases, the message and parity bits of α codewords in all the rows will not be properly aligned in the same column resulting in full rank.

Estimation of n and k:

After substituting $b = \alpha.n$ in (10), the rank ratio values for convolutional and block codes are given by (11) and (12), respectively. From proposition 2, n can be identified by observing the difference between two successive rank deficient columns. Let $b = \alpha.n$ and $b' = (\alpha + 1).n$ indicate the two rank deficient columns for the case without interleaver and the difference $b' - b$ gives the value of n. In addition, the code dimension k can also be identified by observing the difference between two successive rank values $\rho(S)$ and $\rho'(S)$ corresponding to b and b', respectively. We know that for convolutional codes $\rho'(S) = (\alpha+1).k+m$ and $\rho(S) = \alpha.k+m$. Similarly, for block codes $\rho'(S) = (\alpha + 1).k$ and $\rho(S) = \alpha.k$. Now the difference $\rho'(S) - \rho(S)$ gives the value of k.

Proposition 3: Uncoded case

If S is a data matrix of uncoded symbols with b columns, then $\rho(S) = b$, the full rank of the data matrix.

Proof:

Since the incoming uncoded data symbols are independent of each other, full rank will be obtained irrespective of the values of b.

Code classification:

Therefore, the incoming data symbols with or without interleaver can be classified easily from the rank ratio equations of convolutional and block codes, which are given by (11) and (12), respectively. From (11), it can be inferred that the deficient rank ratio will be much greater than r for lower values of b. As b increases, the deficient rank ratio will tend to remain constant slightly above r, since λ will be negligible compared to r and it will not be equal to zero. Therefore, for convolutional codes with or without block interleaver, the deficient rank ratio will decay rapidly for smaller values of b and for larger values of b, it will approximately remain constant slightly above r. However, from (12), it can be inferred that the deficient rank ratio will remain constant at r for block codes with or without block interleaver. Finally, it can be observed from proposition 3 that p will remain constant at unity for all values of b considering the uncoded data symbols.

IV. CODE CLASSIFICATION AND INTERLEAVER PERIOD ESTIMATION OVER NOISY TRANSMISSION ENVIRONMENT

The methodology proposed for calculating $\rho(S)$ and p in the previous section is restricted to ideal non-erroneous case. It is to be noted that for non-erroneous or error-free scenario, all the dependent columns will be transformed into all-zero columns after converting S into F. The number of non-zero or independent columns will give the rank value. But for erroneous case, the dependent columns will not get transformed into all-zero columns due to erroneous bits. Therefore, this will lead

to full rank for all values of b irrespective of the type of error correcting codes and hence, code classification will be difficult. Instead of evaluating the number of non-zero columns in F to calculate p, the mean value of the number of ones or zeros in each column of F for a particular value of b is evaluated. This is because, if c^{th} column is dependent, then the mean value of the number of ones in that particular column will be smaller compared to the independent columns. Similarly, the mean value of the number of zeros in c^{th} dependent column will be greater compared to the independent columns. Hence, by calculating the number of independent columns for a particular value of b, $\rho(S)$ and p are evaluated and a detailed algorithm is given as follows:

Algorithm 1:

Input:
data: Coded data symbols
num_data: Number of received coded data symbols
Output: $\rho(S)$ and p

- Step:1 Initialize: *data*, *num_data*, b [2], and a [3] such that $num\_data > a.b$.
- Step:2 Compute the number of frames, which is given by $N_{\text{frame}} = \text{floor}(num\_data/b)$ and initialize $N = N_{\text{frame}} - a + 1$.
- Step:3
  For $j = 1 : N$
  $R_j \leftarrow data(1 + (j-1)b \; : \; ba + (j-1)b)$
  $S_j \leftarrow$ reshape R_j with b columns and a rows
  $F_j \leftarrow S_j \times \chi_j$
  $A_j \leftarrow$ compute $\omega_j(c)$ or $\delta_j(c)$ for each column in F_j, where $c \in \{1, 2, ..., b\}$
  end For
- Step:4 Compute $mean(A)$, where $A = [A_1 A_2 A_3 \cdots A_N]^T$, $A_j = [\omega_j(1)\omega_j(2)\cdots\omega_j(b)]$ or $A_j = [\delta_j(1)\delta_j(2)\cdots\delta_j(b)]$, and $mean(A) = [\lambda(1)\lambda(2)\cdots\lambda(b)]$ is a row vector of size $1 \times b$, and $\lambda(c) = \frac{\sum_{j=1}^{N} \omega_j(c)}{N}$ or $\lambda(c) = \frac{\sum_{j=1}^{N} \delta_j(c)}{N}$
- Step:5
  If A_j **is computed based on** $\omega_j(c)$
  $\rho(S) \leftarrow$ **card** $\left(c \in \{1, 2, ..., b\} \mid \lambda(c) < \Gamma_{\text{opt}}^{\text{th}}\right)$
  else If A_j **is computed based on** $\delta_j(c)$
  $\rho(S) \leftarrow$ **card** $\left(c \in \{1, 2, ..., b\} \mid \lambda(c) > \Gamma_{\text{opt}}^{\text{th}}\right)$
  end If
- Step:6 Compute $p = \frac{\rho(S)}{b}$

Note that in step 3 of algorithm 1, the data matrix S_j is converted into column echelon form F_j using modified GJETP process, where χ_j denotes the column permutation matrix of size $b \times b$. From step 3, j denotes the index number of data matrix S_j of size $a \times b$, $\omega_j(c) = \phi_j(c)/a$, $\delta_j(c) = \bar{\phi}_j(c)/a$, $\phi_j(c)$ and $\bar{\phi}_j(c)$ denote the number of ones and zeros in c^{th} column of F_j, respectively, and $\Gamma_{\text{opt}}^{\text{th}}$ represents the optimal threshold value. Using step 5, $\rho(S)$ and p are calculated by varying b and **card**$(\cdot)$ in step 5 denotes the cardinality operation. After finding $\rho(S)$ and p, the interleaver period β and code parameters n and k can be estimated as mentioned in Section III. The propositions given in Section III will still hold true to classify the incoming data symbols. Further, two different methodologies are proposed for fixing $\Gamma_{\text{opt}}^{\text{th}}$ to segregate the dependent and independent columns. In the first method, a theoretical expression for $\Gamma_{\text{opt}}^{\text{th}}$ is derived. In the case of second methodology, $\Gamma_{\text{opt}}^{\text{th}}$ is fixed using histogram technique. The analytical and histogram approaches are discussed, respectively, in Section IV.A and IV.B.

[2]Preferably, b should be fixed as a multiple of β or lcm(n, β) for the case with interleaver or n for the case without interleaver to observe the rank deficiency

[3]Fix a such that $a \geq k_1.b$

A. Analytical approach:

An optimal threshold value $\Gamma_{\text{opt}}^{\text{th}}$ is required for the accurate classification of dependent and independent columns. In this section, a theoretical expression for $\Gamma_{\text{opt}}^{\text{th}}$ is derived. In the case of non-erroneous scenario, we know that the dependent columns in S will be transformed into all-zero columns in F. Hence, the columns in permutation matrix χ corresponding to all-zero columns in F can be termed as kernel of S, since $S.d = 0$, where $d = [d_1 d_2 \cdots d_b]^T$ indicates a column vector in χ corresponding to an all-zero column in F. Moreover, the XOR of the column elements in S with column index i corresponding to $d_i = 1$ is equal to 0. Otherwise, there should be even number of ones in the column positions of S corresponding to $d_i = 1$, such that $S.d = 0$. We also know that the dependent columns will not get transformed into all-zero columns in the case of erroneous scenario and hence, ones will appear in some row positions of F instead of zeros depending upon the bit error rate (BER) value. Otherwise, in the case of erroneous scenario, the XOR of the column elements in S with index i corresponding to $d_i = 1$ will not be equal to zero due to odd number of ones. Therefore, the number of ones $\phi_j(c)$ in c^{th} dependent column of F_j is a random variable (RV) denoted by B_c^j and it follows a binomial distribution with parameters a and P_c^j (i.e. $B_c^j \sim \mathcal{B}(a, P_c^j)$), where a indicates the number of rows and P_c^j denotes the probability of getting ones in c^{th} dependent column of F_j. It is given by [6, eq.(11)]

$$\begin{aligned} P_c^j &= 1 - \sum_{l=0}^{\left\lfloor \frac{z_j^c}{2} \right\rfloor} \binom{z_j^c}{2l} p_e^{2l} (1-p_e)^{z_j^c - 2l} \\ &= \frac{1 - (1-2\,p_e)^{z_j^c}}{2}, \end{aligned} \tag{18}$$

where z_j^c denotes the hamming weight of c^{th} column in column permutation matrix χ_j and p_e denotes the BER value. Note that the probability of getting even number of erroneous bits in column positions of S_j corresponding to $d_i = 1$ or the probability of getting zeros in c^{th} dependent column of F_j is given by

$$\bar{P_c^j} = \sum_{l=0}^{\left\lfloor \frac{z_j^c}{2} \right\rfloor} \binom{z_j^c}{2l} p_e^{2l} (1-p_e)^{z_j^c - 2l} \tag{19}$$

It is to be noted that binary symmetric channel (BSC) model is assumed for calculating the threshold value. Similarly, the number of ones $\phi_j(k)$ in k^{th} independent column of F_j is also a RV denoted by D_k^j and it follows $\mathcal{B}(a, P_k^{''})$. Since the probability of ones and zeros appearing in an independent column is equally likely, $P_k^{''}=0.5$. For larger values of a, it is a known fact that the binomial RVs B_c^j and D_k^j can be approximated as normal RVs. Therefore, $B_c^j \sim \mathcal{N}(a.P_c^j, a.P_c^j.(1-P_c^j))$ and $D_k^j \sim \mathcal{N}(\frac{a}{2}, \frac{a}{4})$, where $\mathcal{N}(\mu, \sigma^2)$ denotes the normal distribution with mean μ and variance σ^2.

The mean value of N different normal RVs B_c^j, where $N = N_{\text{frame}} - a + 1$ and $j \in \{1, 2, \cdots, N\}$, is also a RV which is denoted by μ_c. Moreover, μ_c also follows normal distribution with mean and variance given by $\frac{a\,q}{N}$ and $\frac{a\,r}{N^2}$, respectively, where $q = \sum_{j=1}^{N} P_c^j$ and $r = \sum_{j=1}^{N} P_c^j.(1-P_c^j)$. Similarly, the mean value of N different normal RVs D_k^j, which is denoted by μ_k', also follows normal distribution with mean and variance given by $\frac{a}{2}$ and $\frac{a}{4N}$, respectively.

The probability of mis-detection of either dependent or independent column is given by

$$\begin{aligned} P_{\text{md}} &= Pr\left(\frac{\mu_c}{a} > \Gamma^{\text{th}} \mid c^{\text{th}}\text{column is dependent}\right) \\ &\quad + Pr\left(\frac{\mu_k'}{a} < \Gamma^{\text{th}} \mid k^{\text{th}}\text{column is independent}\right) \end{aligned} \quad (20)$$

By substituting the normal probability density function (PDF), (20) can be written as

$$\begin{aligned} P_{\text{md}} &= \int_{a\Gamma^{\text{th}}}^{\infty} \frac{N}{\sqrt{2\,\pi\,a\,r}} \exp\left(-\frac{N^2(\mu_c - \frac{a\,q}{N})^2}{2\,a\,r}\right) d\,\mu_c \\ &\quad + \int_{-\infty}^{a\Gamma^{\text{th}}} \frac{\sqrt{2\,N}}{\sqrt{\pi\,a}} \exp\left(-\frac{2\,N(\mu_k' - \frac{a}{2})^2}{a}\right) d\,\mu_k' \end{aligned} \quad (21)$$

The expression for $\Gamma_{\text{opt}}^{\text{th}}$, which minimizes P_{md}, can be derived by differentiating (21) and equating it to zero. After differentiating and equating it to zero, (21) can be written as

$$\frac{\exp\left(\frac{-a(N\,\Gamma^{\text{th}}-q)^2}{2\,r}\right)}{\exp(-2\,N\,a\,(\Gamma^{\text{th}}-0.5)^2)} = 2\sqrt{\frac{r}{N}} \quad (22)$$

After simplification, (22) can be written as

$$\alpha\,(\Gamma^{\text{th}})^2 + 2\,\gamma\,\Gamma^{\text{th}} + \Delta = 0\,, \quad (23)$$

where $\alpha = Na(4r-N)$, $\gamma = Na(q-2r)$, and $\Delta = raN - aq^2 - r\ln\left(\frac{4r}{N}\right)$. As (23) is a quadratic equation, the possible solutions for Γ^{th} are given by

$$\Gamma^{\text{th}} = \frac{-\gamma + \sqrt{\gamma^2 - (\alpha\,\Delta)}}{\alpha} \text{ or } \Gamma^{\text{th}} = \frac{-\gamma - \sqrt{\gamma^2 - (\alpha\,\Delta)}}{\alpha} \quad (24)$$

From (24), it has been observed that the first solution is negative and hence, the relevant or optimal solution for Γ^{th} is given by

$$\Gamma_{\text{opt}}^{\text{th}} = \frac{-\gamma - \sqrt{\gamma^2 - (\alpha\,\Delta)}}{\alpha} \quad (25)$$

For a particular value of b, $\Gamma_{\text{opt}}^{\text{th}}$ is computed for each column. Similarly, $\omega_j(c)$ is computed for each column considering $N = N_{\text{frame}} - a + 1$ data matrices each of size $a \times b$ as mentioned in step 3 of algorithm 1. After that the mean of all N row vectors (i.e. $\lambda(c)$) is evaluated and the same is compared with $\Gamma_{\text{opt}}^{\text{th}}$ to calculate $\rho(S)$ and p as mentioned in step 5 of algorithm 1. It is also to be noted that the exact BER value p_e need not be known to evaluate $\Gamma_{\text{opt}}^{\text{th}}$. We can fix a maximum value for BER $p_e^{\max}$ depending upon the environment and calculate $\Gamma_{\text{opt}}^{\text{th}}$ in algorithm 1 to evaluate $\rho(S)$. The same optimal threshold values work well for the case when $p_e \leq p_e^{\max}$.

B. Histogram approach:

The optimal threshold value $\Gamma_{\text{opt}}^{\text{th}}$ can also be fixed by plotting the histogram for $mean(A)$, where $mean(A) = [\lambda(1)\lambda(2)\cdots\lambda(b)]$ is a row vector of size $1 \times b$, considering particular number of columns b, which result in rank deficiency. Note that in the histogram-based approach, we compute $\lambda(c)$ for each column in F_j, where $c \in \{1, 2, ..., b\}$, based on $\delta_j(c)$. From the histogram plots, a range of possible threshold values, which properly segregate the dependent and independent columns, is obtained. From the range of possible values, a safe optimal threshold value $\Gamma_{\text{opt}}^{\text{th}}$ is fixed. The same optimal threshold value is applicable for all the other values of b to classify the dependent and independent columns. In Section VI, the optimal threshold values considering two different BER values for different test cases are tabulated.

V. Estimation of rest of the block interleaver parameters

After recognizing β or $\text{lcm}(n, \beta)$, rest of the block interleaver parameters N_r and N_c can be estimated using the following algorithm.

Algorithm 2:

Input : $\zeta = \beta$ or $\text{lcm}(n, \beta)$ **Output** : N_r^{est} and N_c^{est}

- Step:1 Fix a maximum value for codeword length $n_{\max}$ depending upon the type of error correcting codes.
- Step:2
  For $i = 1 : n_{\max}$
  Get all possible combinations of N_r' and N_c' that satisfy $N_r' \times N_c' = \frac{\zeta}{i}$
  end For
- Step:3 Fix b as a multiple of ζ.
- Step:4 De-interleave S_j, where $j \in \{1, 2, ..., N_{\text{frame}} - a + 1\}$, with all possible combinations of N_r' and N_c' and evaluate $mean(A) = [\lambda(1)\lambda(2)\cdots\lambda(b)]$ following the same procedure mentioned in Algorithm 1.
- Step:5 Compute the zero mean ratio $\delta'(b)$, which is given by

$$\delta'(b) = \frac{\sum_{c=1}^{b} \lambda(c)}{b}\,, \quad (26)$$

  for all possible combinations of N_r' and N_c'.
- Step:6 Find $[N_r^{\text{est}} N_c^{\text{est}}] = \underset{N_r', N_c'}{\text{argmax}}(\delta'(b))$.

Here, $\lambda(c)$ is computed based on $\delta_j(c)$. Alternatively, it can also be computed based on $\omega_j(c)$, then step 6 should be written as follows: Find $[N_r^{\text{est}} N_c^{\text{est}}] = \underset{N_r', N_c'}{\text{argmin}}(\delta'(b))$.

VI. Simulation Results and Discussions

In this manuscript, the convolutional code is denoted as $C(n,k,Y)[g_1^1,...,g_i^j,...,g_k^n]$, where n and k denote the codeword length and code dimension, respectively, Y indicates the constraint length, and g_i^j represents the generator polynomial between i^{th} input and j^{th} output and is represented in octal form. Further, the linear block code is represented as $B(n,k)$. It is to be noted that the BER values assumed in our simulation studies are after demodulation and before FEC decoding. The focus of the present work is to analyze the performance of the parameter estimation algorithms in noisy transmission environment. The BER at the decoder is a true reflection of this transmission environment. As we know, various transmission standards specify the allowable BER for a given quality of service (QOS). For example, the post-FEC BER requirement for desirable operation of DVB receiver is 2×10^{-4} [31]. Considering the BER values together with the allowances of coding gain, the pre-FEC BER values for acceptable performance will be usually greater than 10^{-3}. Considering these factors, we have taken a safe value of 10^{-2} as the BER threshold to account the worst case scenario. The overall performance of the algorithm is extensively tested within the range of 5×10^{-3} to 6×10^{-2} and the respective results are given in this section.

The simulation results and discussions considering different case studies without and with interleaver are reported in Section VI.A and VI.B, respectively. In Section VI.C, the results and discussions which are valid for both the cases are given. Finally, the observations related to the accuracy of estimation of the proposed algorithms are given in Section VI.D.

A. Simulation results for the case without interleaver:

In Fig. 3(a), the rank ratio plot considering $B(7,4)$ is shown assuming non-erroneous or error-free scenario. From the plot, it is inferred that the deficient rank ratio values remain constant at $r=4/7$. Hence, the incoming coded data symbols can be classified as block coded symbols. Moreover, the difference between the successive number of columns with rank deficiency gives the estimate of $n=7$. In Fig. 3(b), the rank ratio plot for $B(7,4)$ without interleaver is shown for erroneous scenario assuming BER = 5×10^{-3}. Note that the rank values are obtained from the methodology proposed for non-erroneous scenario in Section III. From the figure, it can be observed that irrespective of b, full rank is obtained due to erroneous bits and hence, it is difficult to classify the incoming coded data symbols and estimate n using the methodology proposed for non-erroneous scenario.

In Fig. 4(a), the rank ratio plot is shown for $C(3,1,7)[133,165,171]$ assuming BER = 2×10^{-2}. Based on algorithm 1, the rank ratio values are obtained and based on the histogram approach, $\Gamma_{\text{opt}}^{\text{th}}$ is fixed. It can be observed that the deficient rank ratio decays rapidly for the case when b is a multiple of n and as b increases, the deficient rank ratio tends to remain constant slightly above $r=0.33$. Moreover, for the case when b is not a multiple of n, full rank is obtained. Since the deficient rank ratio is not constant and decays rapidly, the incoming coded data stream can be easily recognized as convolutionally coded data. In Fig. 4(b), the rank ratio plot is shown for $B(6,3)$ considering erroneous scenario assuming BER = 10^{-2}. Since the deficient rank ratio remains constant at $r=0.5$ for the case when $b=\alpha.n$, the incoming coded data stream can be easily identified as block coded data. In addition, it has been observed that for the case when $b\neq\alpha.n$, full rank is obtained. It is also observed from Fig. 4(a) and 4(b) that the difference between the successive number of columns with rank deficiency gives the estimate of n.

In Fig. 5(a) and 5(b), $\rho(S)$ versus b plots are shown for $C(3,1,4)[13,15,17]$ with BER = 2×10^{-2} and $B(7,4)$ with BER = 10^{-2}, respectively. From Fig. 5(a) and Fig. 5(b), it can be observed that the difference between the successive number of columns with rank deficiency gives the corresponding values of codeword lengths i.e. $n=3$ and $n=7$, respectively. Further, code dimensions (i.e. $k=1$ and $k=4$) can be obtained by finding the difference between the successive rank values corresponding to the rank deficient columns. Therefore, by plotting p versus b, code classification can be performed and further, by plotting $\rho(S)$ versus b, code parameters k and n can be estimated.

In Fig. 6(a), the histogram plot for $mean(A)$ considering $b=48$ assuming $C(3,1,7)[133,165,171]$ and BER = 2×10^{-2} is shown. From the plot, it can be inferred that the value of $\lambda(c)$ for 22 columns out of 48 is around 0.5. In addition, for the rest of 26 columns, $\lambda(c)$ is greater than 0.57. Since more than 57% of the elements in 26 columns are zeros, they can be categorized as dependent columns. It is to be noted that these 26 columns should have been all-zero-columns with high probability in the case of non-erroneous scenario. Hence, by fixing $\Gamma_{\text{opt}}^{\text{th}}$ between 0.53 to 0.56, dependent and independent columns can be easily categorized. From Fig. 6(a) and from step 5 of algorithm 1, it can be inferred that $\rho(S)=22$ and $p=0.4583$ for $b=48$, which is also justified in Fig. 4(a). Moreover, $\rho(S)=22$ can also be validated from (16). As $n=3$ and $b=48$, the value of α is equal to 16. Since $m=Y-1$, from (16), $\rho(S)=22$ and $p=0.4583$. The histogram plot for $\lambda(c)$ in each column considering $b=42$ assuming linear block code $B(6,3)$ and BER = 10^{-2} is shown in Fig. 6(b). From the plot, it can be observed that $\rho(S)=21$ and $p=0.5$ by fixing $\Gamma_{\text{opt}}^{\text{th}}$ between 0.55 to 0.7 and the rank values can also be validated using Fig. 4(b) and (17). It is to be noted that the same optimal threshold values obtained from Fig. 6(a) and (b) are fixed for other values of b to classify the dependent and independent columns in order to evaluate $\rho(S)$.

B. Simulation results for the case with interleaver:

In Fig. 7(a) and 7(b), the rank ratio plots for $B(8,5)$ and $C(2,1,4)[15,17]$ with block interleaver are, respectively, shown for erroneous scenario assuming BER = 5×10^{-3}. Here, the rank values are obtained based on algorithm 1 and $\Gamma_{\text{opt}}^{\text{th}}$ is fixed based on (25). From Fig. 7(a), which is shown for the case assuming $N_r=4$ and $N_c=2$, it can be observed that the deficient rank ratio values remain constant at $r=5/8$ and the difference between the successive rank deficient columns gives the estimate of $\beta=N_r\times N_c$. Hence, the incoming

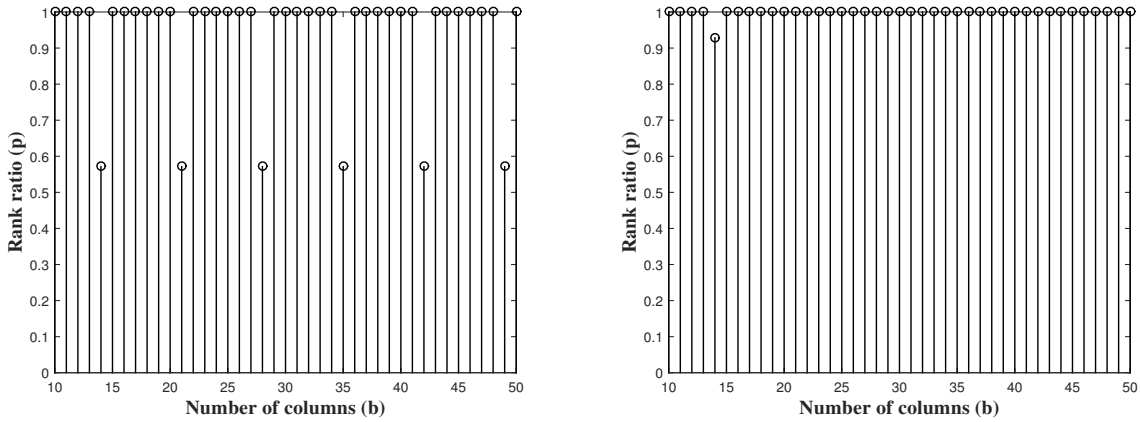

(a) (b)

Fig. 3. (a) Variation of rank ratio p with b for $B(7,4)$ assuming BER = 0. (b) Variation of rank ratio p with b for $B(7,4)$ assuming BER = 5×10^{-3}

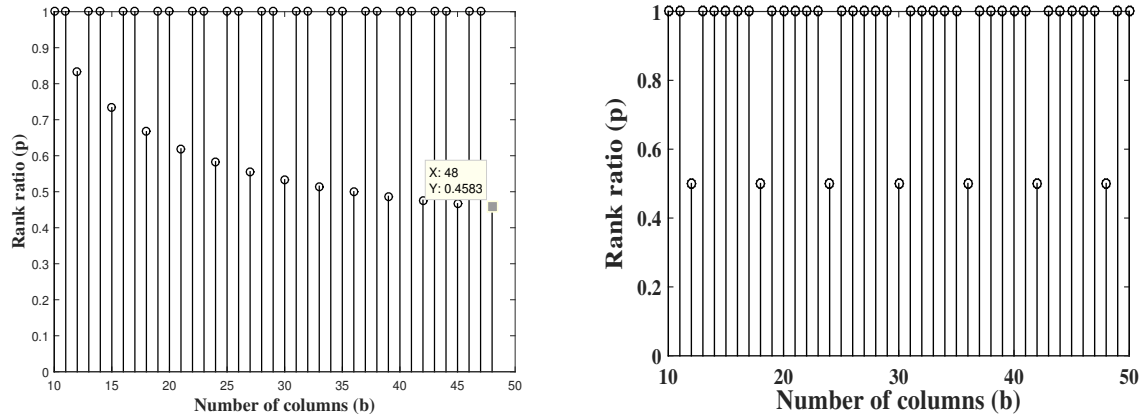

(a) (b)

Fig. 4. (a) Rank ratio p versus number of columns b for $C(3,1,7)[133,165,171]$ with BER = 2×10^{-2}. (b) Rank ratio p versus number of columns b for $B(6,3)$ with BER = 10^{-2}.

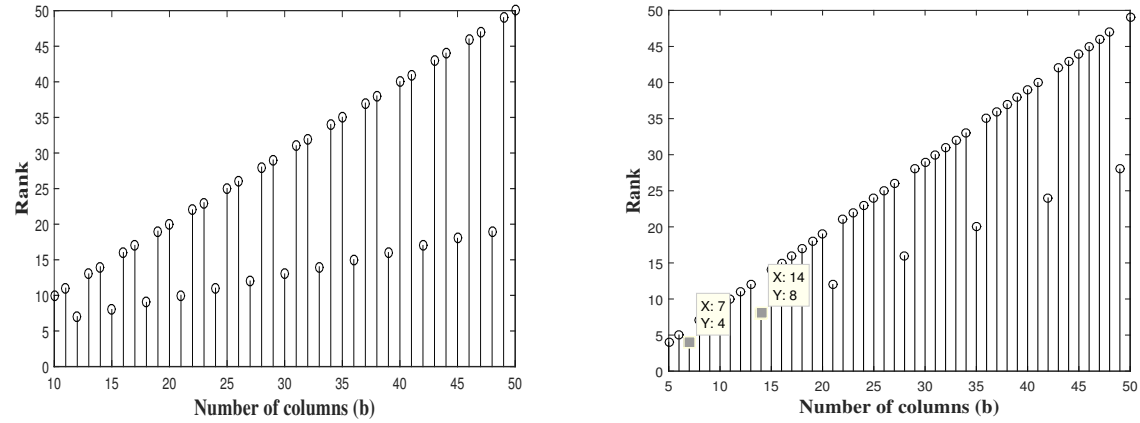

(a) (b)

Fig. 5. (a) Rank $\rho(S)$ versus number of columns b for $C(3,1,4)[13,15,17]$ with BER = 2×10^{-2}. (b) Rank $\rho(S)$ versus number of columns b for $B(7,4)$ with BER = 10^{-2}.

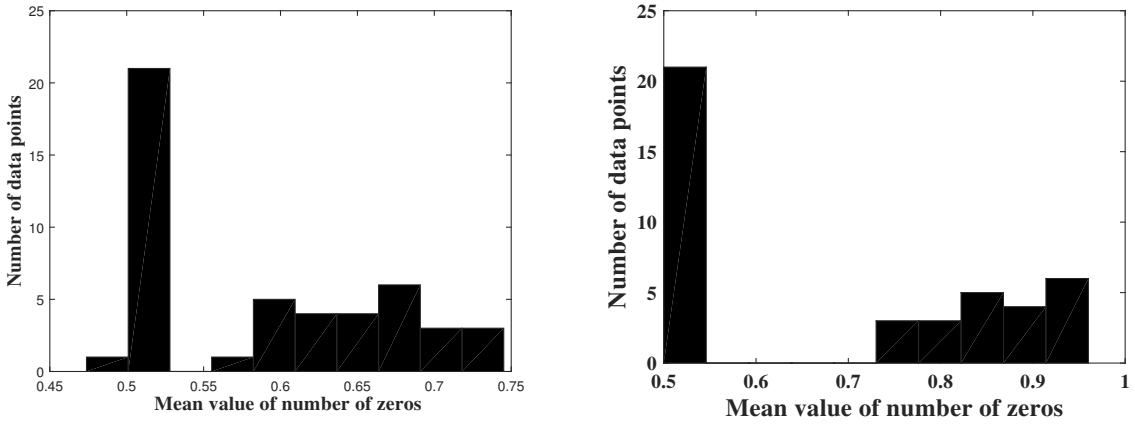

(a) (b)

Fig. 6. (a) Histogram plot for $mean(A)$ considering $b=48$, $C(3,1,7)[133,165,171]$, and BER = 2×10^{-2}. (b) Histogram plot for $mean(A)$ considering $b=42$, $B(6,3)$, and BER = 10^{-2}

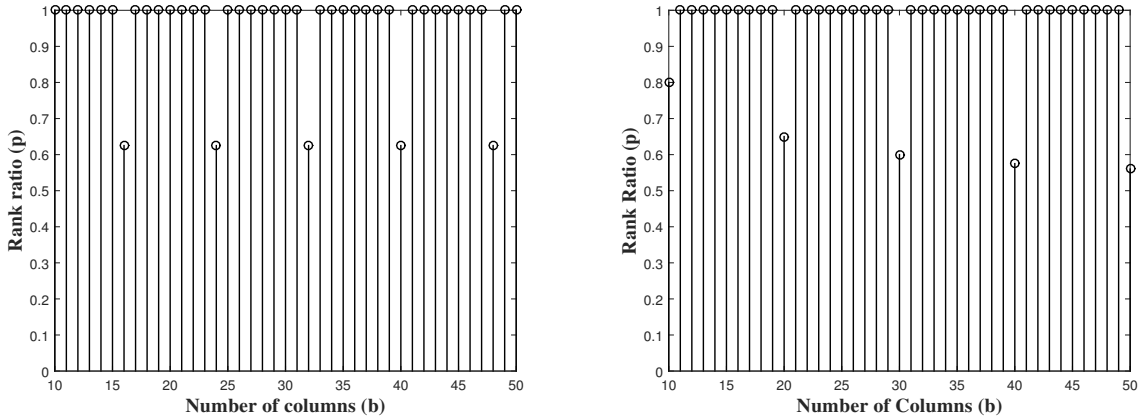

(a) (b)

Fig. 7. (a) Variation of rank ratio p with b for $B(8,5)$ considering block interleaver assuming BER = 5×10^{-3}, $N_r=4$, and $N_c=2$. (b) Variation of rank ratio p with b for $C(2,1,4)[15,17]$ considering block interleaver assuming BER = 5×10^{-3}, $N_r=5$, and $N_c=2$

coded data symbols can be successfully classified as block coded symbols and β has also been estimated successfully over erroneous scenario. From Fig. 7(b), which is shown for the case assuming $N_r = 5$ and $N_c = 2$, it can be observed that the deficient rank ratio values decay for lower values of b. Further, it tends to remain constant above $r=0.5$ for higher values of b. Hence, the incoming erroneous data symbols can be classified as convolutionally coded symbols. By observing the difference between the successive rank deficient columns, $\beta=10$ (i.e. $N_r \times N_c$) can be identified successfully.

In Fig. 8(a), the rank ratio plot is shown for $B(6,3)$ considering block interleaver with $N_r=3$, $N_c=3$, and BER = 10^{-2}. Here, the histogram approach is used for fixing $\Gamma^{\text{th}}_{\text{opt}}$. From the figure, it is inferred that the deficient rank ratio values remain constant at $r = 0.5$ for the case when b is a multiple of 18 (i.e. lcm(n,β)). Therefore, the incoming data symbols can be recognized as block coded symbols. From the figure, it is also observed that the difference between the successive number of columns with rank deficiency is equal to 18 (i.e. lcm(n,β)). It is to be noted that for the case when β is a multiple of n (refer Fig. 7(a)), the difference between the rank deficient columns gives the estimate of β. But for the case when β is not a multiple of n, the column difference gives the estimate of lcm(n,β). In Fig. 8(b), the variation of $\delta'(b)$ is shown for all possible combinations of N'_r and N'_c that satisfy $N'_r \times N'_c = \frac{\zeta}{i}$ as mentioned in algorithm 2. From the plot, it is observed that $\delta'(b)$ is maximum for $N'_r=3$ and $N'_c=3$, which gives the correct estimate of block interleaver parameters in a noisy transmission environment.

In Fig. 9(a), the rank ratio plot is shown for $C(3,1,7)[133,165,171]$ considering block interleaver with $N_r = 4$, $N_c = 3$, and BER = 2×10^{-2}. Here, the histogram approach is used for fixing $\Gamma^{\text{th}}_{\text{opt}}$. From the figure, it can be observed that initially, the deficient rank ratio values decay rapidly for the case when b is a multiple of $\beta=12$ and as b increases, it tends to remain constant slightly above the code rate value of 1/3. As the deficient rank ratio values are not constant, the incoming coded data symbols can be easily classified as convolutionally coded symbols. Moreover, from the plot it can also be observed that the column difference between the successive columns with rank deficiency gives the correct estimate of β. In Fig. 9(b), the variation of zero

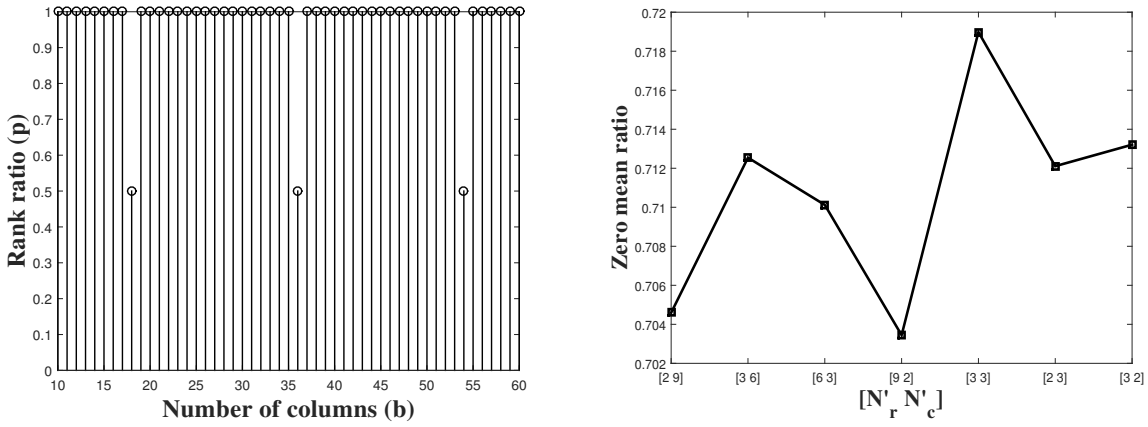

(a) (b)

Fig. 8. (a) Variation of rank ratio p with b for $B(6,3)$ considering block interleaver assuming $N_r=3$, $N_c=3$, and BER = 10^{-2}. (b) Variation of zero mean ratio $\delta'(b)$ with all possible values of $[N'_r\ N'_c]$ for $B(6,3)$ considering block interleaver assuming $N_r=3$, $N_c=3$, and BER = 10^{-2}.

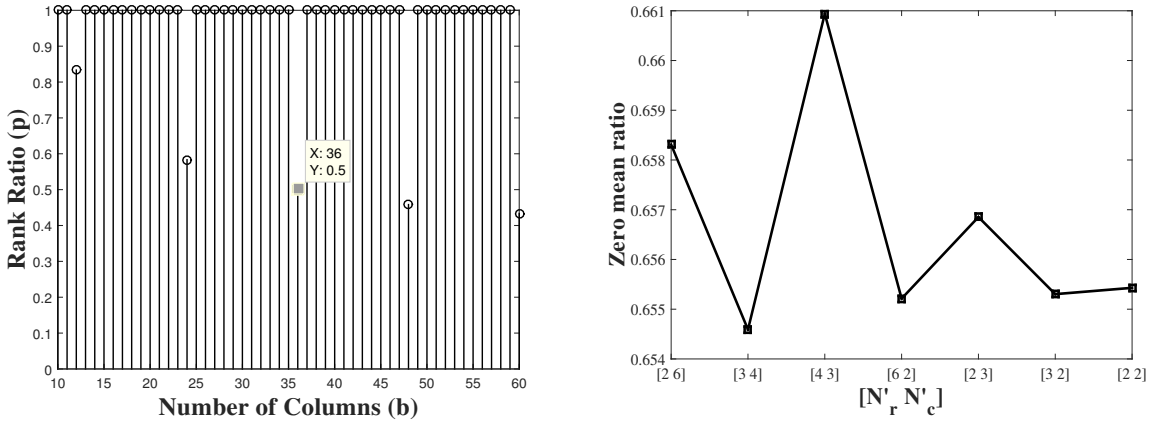

(a) (b)

Fig. 9. (a) Variation of rank ratio p with b for $C(3,1,7)[133,165,171]$ considering block interleaver assuming $N_r=4$, $N_c=3$, and BER = 2×10^{-2}. (b) Variation of zero mean ratio $\delta'(b)$ with all possible values of $[N'_r\ N'_c]$ for $C(3,1,7)[133,165,171]$ considering block interleaver assuming $N_r=4$, $N_c=3$, and BER = 2×10^{-2}.

mean ratio $\delta'(b)$ for all possible values of $[N'_r\ N'_c]$ considering the same case is shown. As mentioned in algorithm 2, $\delta'(b)$ is evaluated by de-interleaving with all possible combinations of N'_r and N'_c that satisfy $N'_r \times N'_c = \frac{\zeta}{i}$. From the plot, it can be inferred that for $[N'_r\ N'_c] = [4\ 3]$, the zero mean ratio curve reaches maximum and hence, the interleaver parameters are estimated successfully.

It is to be noted that for the case with interleaver, code parameters n and k can be obtained from $\rho(S)$ versus b plot after de-interleaving using the estimated interleaver parameters.

In Fig. 10(a), the histogram plot for $mean(A)$ is shown assuming $N_r=4$, $N_c=3$, $b=36$, $C(3,1,7)[133,165,171]$, and BER = 2×10^{-2}. From the plot, it can be observed that the value of $\lambda(c)$ for 18 columns out of 36 columns is in between 0.5 to 0.52. Moreover, for the rest of 18 columns, $\lambda(c)$ is greater than 60% and therefore, they can be categorized as dependent columns. Note that these 18 columns with $\lambda(c)$ greater than 60% should have been all-zero columns, if no errors were introduced. Therefore, by setting an optimal threshold value $\Gamma^{\text{th}}_{\text{opt}}$ between 0.53 to 0.59, the dependent and independent columns can be classified. Since the number of independent columns define the rank of a matrix, from Fig. 10(a) and from step 5 of algorithm 1, it can be inferred that $\rho(S)=18$ and the same is also validated in Fig. 9(a), as $p=18/36=0.5$ for the case when $b=36$. In addition, the rank value can also be justified by evaluating $\rho(S)$ given by (2). Since $n=3$ and $b=36$, the value of α and γ will be equal to 3 and 4, respectively. As $m=K-1$, $\rho(S)=18$ from (2) and $p=0.5$.

In Fig. 10(b), the histogram for $mean(A)$ is shown considering $N_r=3$, $N_c=3$, $b=36$, $B(6,3)$, and BER = 10^{-2}. It can be inferred from the figure that $\lambda(c)$ for 18 columns is in between 0.5 to 0.53 and for the rest of 18 columns it is greater than 0.72. Hence, by setting $\Gamma^{\text{th}}_{\text{opt}}$ between 0.54 to 0.7, the dependent and independent columns can be classified. From Fig. 10(b) and step 5 of algorithm 1, it can be observed that $\rho(S)=18$ and the same is also validated in Fig. 8(a), as $p=18/36=0.5$ for the case when $b=36$.

The same optimal threshold values obtained from Fig. 10(a) and (b) are fixed for other values of b to classify the dependent and independent columns in order to evaluate $\rho(S)$.

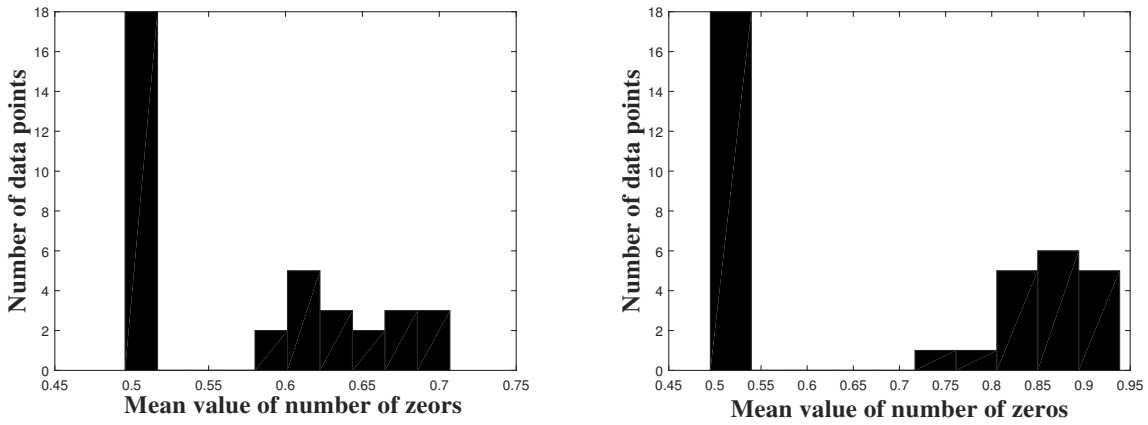

(a) (b)

Fig. 10. (a) Histogram plot for $mean(A)$ assuming $b = 36$, $N_r = 4$, $N_c = 3$, $C(3, 1, 7)[133, 165, 171]$, and BER = 2×10^{-2}. (b) Histogram plot for $mean(A)$ assuming $b = 36$, $N_r = 3$, $N_c = 3$, $B(6, 3)$, and BER = 10^{-2}.

TABLE II
THRESHOLD VALUES $\Gamma^{\text{TH}}_{\text{OPT}}$ FOR VARIOUS TEST CASES

BER	FEC codes	Number of rows	Γ^{th}
10^{-2}	C[2,1,3], C[2,1,4] C[2,1,5], C[2,1,6] C[2,1,7], C[3,1,4] C[3,1,7], C[3,1,11] C[4,1,7], C[4,1,10] B(8,5), B(7,4) B(6,3), B(3,2)	$a = 20 \times b$	0.55
2×10^{-2}	C[2,1,3], C[2,1,4] C[2,1,5], C[3,1,4] C[3,1,7], C[4,1,7] C[4,1,10] B(8,5), B(7,4) B(6,3), B(3,2)	$a = 20 \times b$	0.55
	C[2,1,6], C[3,1,11]	$a = 50 \times b$	0.52
	C[2,1,7]	$a = 70 \times b$	0.51

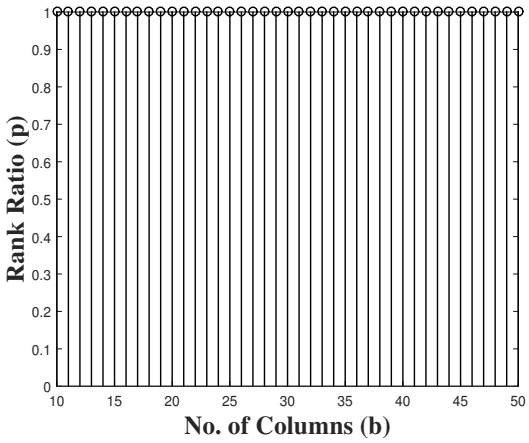

Fig. 11. Variation of rank ratio p with b for uncoded data stream assuming BER = 10^{-2}

C. Results and discussions applicable to both the cases:

The simulation results and related discussions reported here are valid for both the cases (i.e. with and without interleaver). From the histogram plots reported in the previous two sub-sections, it can be also observed that as the BER decreases, $\lambda(c)$ for dependent columns also increases as expected due to less number of erroneous bits. Therefore, the range for choosing $\Gamma^{\text{th}}_{\text{opt}}$ to segregate the dependent and independent columns also widens. Moreover, it is also intuitive that as the BER increases, the range for choosing $\Gamma^{\text{th}}_{\text{opt}}$ decreases and incorrect $\Gamma^{\text{th}}_{\text{opt}}$ value will change the rank ratio characteristics of the block and convolutional codes. From the range of optimal threshold values, a safe value is fixed to classify the dependent and independent columns. In Table II, the safe optimal threshold values $\Gamma^{\text{th}}_{\text{opt}}$ for different test cases are given. From the tabulated values, it has been inferred that as Y and BER increases, the number of rows of S required for successful estimation of $\rho(S)$ also increases and thus, more data size will be required.

In Fig. 11, the variation of p with b is shown for uncoded data symbols assuming BER = 10^{-2}. It can be observed from the figure that the rank ratio remains constant at unity and is independent of b with or without interleaver. Therefore, according to proposition 3, the incoming data symbols can be classified as uncoded.

D. Accuracy of estimation:

From the simulation studies, it is inferred that if the histogram technique is used for fixing $\Gamma^{\text{th}}_{\text{opt}}$, then the code classification technique holds good with 100% accuracy until BER of 2×10^{-2} for the case with interleaver. It can be also observed that for the case when BER $> 2 \times 10^{-2}$, the proposed methodology fails to classify the incoming data symbols among block and convolutional codes, since unique rank ratio characteristics will change drastically due to more number of erroneous bits. However, the estimation of β or lcm(n, β), N_r, and N_c are observed to be successful until BER of 6×10^{-2} for most of the test cases given in Table II. For example, in Fig. 12(a), the rank ratio characteristics for $B(8, 5)$ considering block interleaver with $N_r = 4$ and $N_c = 4$ assuming BER = 6×10^{-2} is shown. Though the rank ratio values are not constant at $r = 5/8$, the difference

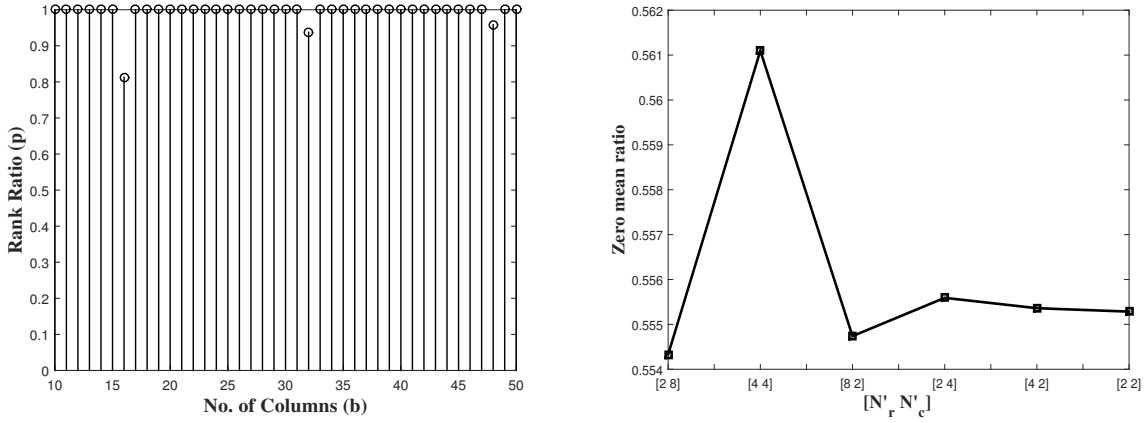

(a) (b)

Fig. 12. (a) Variation of rank ratio p with b for $B(8,5)$ considering block interleaver assuming $N_r=4$, $N_c=4$, and BER = 6×10^{-2}. (b) Variation of zero mean ratio $\delta'(b)$ with all possible values of $[N'_r\ \ N'_c]$ for $B(8,5)$ considering block interleaver with $N_r=4$, $N_c=4$, and BER = 6×10^{-2}

between the successive columns with rank deficiency gives the correct estimate of $\beta=16$. Therefore, the incoming coded symbols with BER = 6×10^{-2} cannot be classified as either block or convolutional codes, however, β can be estimated successfully. Moreover, in Fig. 12(b), the variation of $\delta'(b)$ is shown for all possible values of N'_r and N'_c that satisfy $N'_r \times N'_c = \frac{\zeta}{i}$ as mentioned in algorithm 2. From the plot, it can be observed that $\delta'(b)$ is maximum for $N'_r=4$ and $N'_c=4$ and it gives the correct estimate of interleaver parameters in a noisy transmission environment. For erroneous case with BER $> 6\times10^{-2}$, the proposed algorithm based on the histogram approach fails to recognize the interleaver parameters for most of the test cases given in Table II. Further, it has been observed that for the case without interleaver, the histogram approach fails to recognize the type of FEC codes for BER $> 4\times10^{-2}$.

It is also observed that if $\Gamma^{\text{th}}_{\text{opt}}$ is fixed based on (25), then the type of FEC codes can be estimated with 100% accuracy until BER of 5×10^{-3}. For erroneous case with BER $> 5\times10^{-3}$, $\Gamma^{\text{th}}_{\text{opt}}$ fixed based on the analytical approach fails to classify the incoming coded data symbols. However, β or lcm(n,β), N_r, and N_c can be estimated correctly until BER of 2×10^{-2}.

In Table III, the comparison of accuracy of estimation of detecting the number of dependent columns is shown for block interleaver with $N_r=4$, $N_c=3$, $b=48$, and BER = 10^{-2}. Since $\beta=12$, we know that the rank deficiency will be obtained for the case when $b=48$. According to (3), $\rho(S)=26$ considering $C(2,1,3)$ and hence, the number of dependent columns is equal to 22 as given in Table III. Similarly, we can obtain the number of dependent columns for other test cases. Here, we have compared the accuracy of estimation of the dependent columns considering three different methodologies for fixing $\Gamma^{\text{th}}_{\text{opt}}$. In the first methodology, $\Gamma^{\text{th}}_{\text{opt}}$ is fixed based on [6, eq.(A.4)]. For the second and third methodologies, we have fixed $\Gamma^{\text{th}}_{\text{opt}}$ based on (25) and histogram approach, respectively. From the tabulated values, it can be noted that the accuracy of estimation is better if $\Gamma^{\text{th}}_{\text{opt}}$ is fixed based on the analytical approach using (25) compared to [6, eq.(A.4)] for lower values of Y. It is also noticed that the proposed histogram approach

TABLE III
COMPARISON OF ACCURACY OF ESTIMATION OF DIFFERENT METHODOLOGIES

Test case	Actual No. of dependent columns for $b=48$	Estimated number of dependent columns for $b=48$ (% of Accuracy)		
		Fixing $\Gamma^{\text{th}}_{\text{opt}}$ based on (25)	Fixing $\Gamma^{\text{th}}_{\text{opt}}$ based on [6, eq.(A.4)]	Fixing $\Gamma^{\text{th}}_{\text{opt}}$ based on histogram approach
C(2,1,3)	22	19 (86.4%)	15 (68.2%)	22 (100%)
C(2,1,4)	21	17 (81%)	17 (81%)	21 (100%)
C(3,1,4)	29	28 (96.6%)	26 (89.7%)	29 (100%)
C(3,1,7)	26	23 (88.5%)	23 (88.5%)	26 (100%)
C(3,1,10)	23	16 (82.6%)	16 (82.6%)	23 (100%)
C(4,1,7)	30	29 (96.7%)	26 (86.7%)	30 (100%)

performs better than the other two methodologies irrespective of Y.

It is to be observed that the distribution of mean value of number of zeros in each columns has been predicted accurately in the histogram approach. In the analytical approach, we have approximated the binomial distribution of mean value of number of zeros to normal distribution. This is because, it is very difficult to get a closed-form expression for $\Gamma^{\text{th}}_{\text{opt}}$ using binomial distribution. Therefore, the performance degradation of the analytical method compared to the histogram method is mainly due to the approximation of binomial to normal distribution for evaluating $\Gamma^{\text{th}}_{\text{opt}}$.

The expression for $\Gamma^{\text{th}}_{\text{opt}}$ in [6] is derived considering a single data matrix S and the estimation performance improves with the number of iterations. However, in the proposed work, we derive $\Gamma^{\text{th}}_{\text{opt}}$ by considering $N = N_{\text{frame}} + a - 1$ data matrices as given in step 3 of algorithm 1. Note that all the

three methodologies are compared by keeping the computation time constant. Even though the histogram approach for fixing $\Gamma_{\text{opt}}^{\text{th}}$ performs better than the analytical approach, latency should be compromised to achieve better performance. This is because, $\Gamma_{\text{opt}}^{\text{th}}$ can be fixed using the histogram approach only after receiving the entire coded data symbols. However, in the case of analytical approach, $\Gamma_{\text{opt}}^{\text{th}}$ can be fixed on a real time basis while receiving the incoming coded data symbols.

The proposed blind estimation technique based on the rank deficiency can also be extended to LDPC codes or any other FEC codes with larger codeword length. However, the estimation of sparse H matrix is difficult as the matrix size is huge in the case of LDPC codes. Moreover, it has also been observed that the accuracy of estimation of rank-deficiency-based algorithm deteriorates as n increases. Hence, based on the average LLR values of syndrome a posteriori probability [19], the code parameters can be estimated with better accuracy. It is to be noted that in practice, the AMC transceivers would not change the encoder parameters arbitrarily. Therefore, a predefined LDPC encoder candidate set is assumed to be known at both transmitter and receiver and the true encoder is identified based on the average LLR values.

VII. Conclusions

In this paper, the code classification and block interleaver period estimation techniques are proposed for ideal and noisy transmission environments. Further, the analytical and histogram approaches are suggested for setting the optimal threshold value to evaluate rank $\rho(S)$ and rank ratio p. The necessary interleaver parameters are estimated based on the zero mean ratio values. Extensive simulation studies are conducted to evaluate the performance of the proposed algorithm. It has been observed that if the optimal threshold value is fixed based on the proposed analytical approach, then the code classification can be performed successfully until BER of 5×10^{-3} and the interleaver parameters can be estimated successfully until BER of 2×10^{-2}. On the other hand, the respective performances of the histogram approach are 2×10^{-2} and 6×10^{-2}. The results from these studies show that the proposed histogram approach is more robust against the analytical approach for noisy transmission environment. However, one of the important challenges to achieve better performance for the histogram approach is the system latency.

Appendix A
Case study 1: Convolutional code with block interleaver

In this Appendix, the reason for rank deficiency in the case of convolutional codes has been explained using an example. Fig. 13 shows the variation of $\rho(S)$ with b for systematic convolutional encoder $C(2,1,3)[4,7]$ assuming block interleaver with $N_r=3$ and $N_c=2$. In the case of systematic encoder, it is known that k output bits are exact replicas of k input bits. Let us assume that the input sequence $(t_1,t_2,t_3,\cdots)$ enters the systematic rate 1/2 convolutional encoder $C(2,1,3)[4,7]$ one bit at a time. The encoder output codeword sequence is given by $(t_1,g_1,t_2,g_2,t_3,g_3,\cdots)$, where g_i denotes the

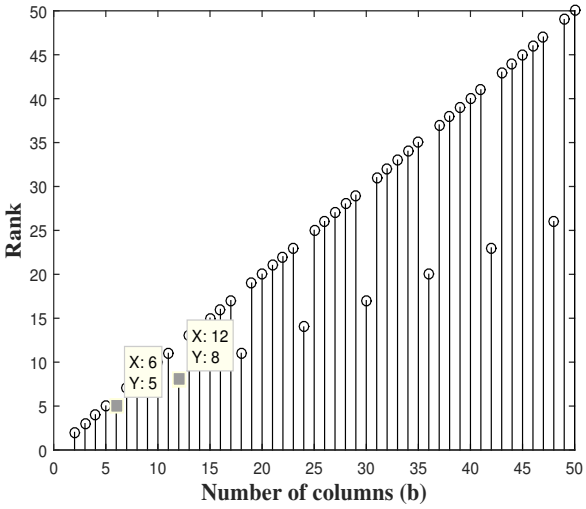

Fig. 13. Variation of rank with number of columns (b) for convolutional code with block interleaver ($C(2,1,3)[4,7]$, $N_r=3$, $N_c=2$)

parity bit corresponding to t_i. After block interleaving the convolutionally coded bits, it has been reshaped into a matrix S of size $a\times b$ assuming $b=6,8,$ and, 12 with number of rows $a=3$ as shown in Table IV. It is to be noted that the matrix-based block interleaver operation is carried out as shown in Fig. 1. For better understanding, only three rows of the block interleaved codewords are shown considering non-erroneous and synchronized case. From the interleaved data stream, three complete codewords (i.e. t_1,g_1,t_2,g_2,t_3,g_3) are observed in all the three rows for the case when $b=6$. It is also noticed that the data and parity bits of all the three codewords are aligned properly in the same column. We know that for a convolutional code, a codeword of length n bits depend on $k+m$ information bits, which consist of k present and m previous input bits introduced by the encoder as mentioned in [2] and [11]. Hence, $\alpha.\gamma.n$ output bits should depend on $\alpha.\gamma.k$ present input and m previous input bits.

In Table IV, the case study is shown by considering interleaver period $\beta=\gamma.n=6$. Note that $\alpha=1$ and $\gamma=3$ for the case when $b=\alpha.\beta=6$. Therefore, as stated before, $\alpha.\gamma.n=6$ output data bits in a particular row will depend on $\alpha.\gamma.k=3$ present and $m=2$ previous input bits. Now the block interleaved data matrix S will be converted into column echelon form F through modified GJETP algorithm as indicated in step 3 of Section III. Since all the data and parity bits are aligned properly in the same column as shown in Table IV, $b=6$ columns will be converted into $\alpha.\gamma.k+m=5$ non-zero or independent columns. It is to be noted that the Gauss-Jordan elimination through pivoting algorithm converts a given matrix into a row or column echelon form by eliminating all the dependent rows or columns [25]. Since the number of independent or non-zero columns in F indicates the rank of the matrix, $\rho(S)$ is given by $\alpha.\gamma.k+m$. Similarly, for the case when $b=12$ (i.e. $\alpha=2$ and $\gamma=3$), six complete codewords are observed in all the three rows and the data and parity bits are aligned properly in the same column. After converting S into F, only $\alpha.\gamma.k+m=8$ non-zero or independent columns

TABLE IV
BLOCK INTERLEAVED DATA STREAM ASSUMING $C(2,1,3)[4,7]$, $N_r=3$ AND $N_c=2$

$b=6$	t_1	t_2	t_3	g_1	g_2	g_3						
	t_4	t_5	t_6	g_4	g_5	g_6						
	t_7	t_8	t_9	g_7	g_8	g_9						
$b=8$	t_1	t_2	t_3	g_1	g_2	g_3	t_4	t_5				
	t_6	g_4	g_5	g_6	t_7	t_8	t_9	g_7				
	g_8	g_9	t_{10}	t_{11}	t_{12}	g_{10}	g_{11}	g_{12}				
$b=12$	t_1	t_2	t_3	g_1	g_2	g_3	t_4	t_5	t_6	g_4	g_5	g_6
	t_7	t_8	t_9	g_7	g_8	g_9	t_{10}	t_{11}	t_{12}	g_{10}	g_{11}	g_{12}
	t_{13}	t_{14}	t_{15}	g_{13}	g_{14}	g_{15}	t_{16}	t_{17}	t_{18}	g_{16}	g_{17}	g_{18}

will be observed resulting in rank deficiency. However, for the case when $b=8$, it can be observed that the data and parity bits are not aligned properly in the same column. Hence, after converting S into F, full rank will be observed. The corresponding rank values obtained for $b=6$ and 12 as shown in Fig. 13 well agree with the expression $\rho(S)=\alpha.\gamma.k+m$ (see (2)). From the figure, it is also observed that the rank deficiency is obtained only when b is a multiple of β (i.e. $b=\alpha.\beta$) and for rest of the values, full rank is noticed. Otherwise, the data and parity bits as shown in Table IV will be aligned properly in the same column only when b is a multiple of β resulting in rank deficiency. For rest of the values, full rank will be obtained due to misalignment of data and parity bits. Moreover, $b_{\text{min}}=6$ is obtained after substituting $\gamma=3$, $n=2$, $k=1$, and $\beta=6$ in (9) and the same is also observed in Fig. 13, as the rank deficiency starts from $b=6$.

It is also to be noted that $\rho(S)$ for non-erroneous case can be obtained from F by counting the number of non-zero columns. However, for erroneous case, it can be obtained from F by evaluating the mean value of number of zeros in each column for a particular value of b.

The above explanation given for the rank deficiency considering convolutional codes can be extended to block codes by assuming $m=0$, since block code is a special case of convolutional code with no memory. Therefore, $\rho(S)=\alpha.\gamma.k$ for block codes when $b=\alpha.\beta$. For rest of the values, full rank will be obtained. The same explanation can also be extended to the case without interleaver by assuming $\gamma=1$.

APPENDIX B
CASE STUDY 2: BLOCK CODE WITHOUT INTERLEAVER

For better understanding, another case study explaining the rank deficiency phenomenon considering block codes without interleaver has been discussed in this Appendix. Let us assume the input sequence $(t_1,t_2,t_3,t_4,\cdots)$ enters the systematic block encoder $B(7,4)$ one bit at a time. The codeword corresponding to the input sequence is given by $(t_1,t_2,t_3,t_4,g_1,g_2,g_3,\cdots)$, where g_1, g_2, and g_3 denote the parity bits corresponding to the input sequence (t_1,t_2,t_3,t_4). Similarly, g_4, g_5, and g_6 denote the parity bits corresponding to the input sequence (t_5,t_6,t_7,t_8). It has been reshaped into a matrix S of size $a\times b$ assuming $b=7,10,\text{and},14$ with number of rows $a=3$ as shown in Table V. From the coded data stream, one and two complete codewords are observed in all the three rows for the case when $b=7$ and $b=14$, respectively. It is also noticed that the data and parity bits are also aligned properly in the same column for both the cases. For a block code, it is obvious that a codeword of length n bits depend only on k information bits. Hence, $\alpha.n$ output bits will depend on $\alpha.k$ input bits. Therefore, after converting S into F, only $\alpha.k=4$ non-zero or independent columns will be observed for the case when $b=7$ and $\alpha.k=8$ independent columns will be observed for the case when $b=14$. Note that $\alpha=1$ for $b=7$ and $\alpha=2$ for $b=14$. The corresponding rank values obtained for $b=7$ and 14 as shown in Fig. 5(b) well agree with the expression $\rho(S)=\alpha.k$ (see (17)). It is also inferred from the figure that the rank deficiency is obtained only when $b=\alpha.n$. This is mainly because of the proper alignment of the data and parity bits in the same column. If $b\neq\alpha.n$, then it can be noticed from Table V that the data and parity bits are not aligned properly in the same column (refer to $b=10$ case) and hence, this will result in full rank as shown in Fig. 5(b).

ACKNOWLEDGMENT

The authors would like to thank anonymous reviewers for providing fruitful suggestions to improve the quality of the manuscript.

REFERENCES

[1] M. Jang, H. Lee, S-H. Kim, S. Myung, H. Jeong, and J. Kim, "Design of LDPC Coded BICM in DVB Broadcasting Systems With Block Permutations," *IEEE Trans. Broadcast.*, vol. 61, no. 2, pp. 327–333, June 2015.

[2] M. Marazin, R. Gautier, and G. Burel, "Dual code method for blind recognition of convolutional encoder for cognitive radio receiver design," *in Proc. IEEE GLOBECOM*, 2009, pp. 1–6.

[3] D. Minoli, "Innovations in satellite communications and satellite technology," New Jersey, USA: John Wiley and Sons, 2015.

[4] T.O. El Shabrawy and S. H. Abdel Wahed, "Adaptive modulation and coding for broadcast DVB-H systems," *in Proc. IEEE PIMRC*, 2009, pp. 1292–1296.

[5] T. Xia, H.-C. Wu, S. Y. Chang, X. Liu, and S. C.-H. Huang, "Blind identification of binary LDPC codes for $M-$QAM signals," *in Proc. IEEE GLOBECOM*, 2014, pp. 3532–3536.

[6] G. Sicot and S. Houcke, "Blind detection of interleaver parameters," *Signal Process.*, vol. 89, pp. 450–462, April 2009.

[7] V. Kuvaja, "Identification of error correction codes in signals intelligence," M.S. thesis, School Elect. Eng., Aalto Univ., Espoo, Finland, 2015.

[8] G. L. Rosen, "Examining coding structure and redundancy in DNA," *IEEE Eng. Med. Biol. Mag.*, vol. 25, no. 1, pp. 62–68, Jan. 2006.

[9] J-P. Tillich, A. Tixier, N. Sendrier, "Recovering the interleaver of an unknown Turbo-Code," *in Proc. IEEE ISIT*, 2014, pp. 2784–2788.

[10] J. Dingel and J. Hagenauer, "Parameter estimation of a convolutional encoder from noisy observations," *in Proc. IEEE ISIT*, 2007, pp. 1776–1780.

[11] M. Marazin, R. Gautier, and G. Burel, "Blind recovery of k/n rate convolutional encoders in a noisy environment," *EURASIP J. Wirel. Commun. and Netw.*, vol. 2011, no. 168, pp. 1–9, 2011.

[12] M. Marazin, R. Gautier, and G. Burel, "Some interesting dual-code properties of convolutional encoder for standards self-recognition," *IET Commun.*, vol. 6, no. 8, pp. 931–935, July 2012.

[13] Y. Zrelli, M. Marazin, R. Gautier, E. Rannou, and E. Radoi, "Blind identification of convolutional encoder parameters over GF(2m) in the noiseless case," *in Proc. IEEE ICCCN*, 2011, pp. 1–5.

TABLE V
BLOCK CODE $B(7,4)$ RESHAPED INTO A DATA MATRIX S OF SIZE $3\times b$

$b=7$	t_1	t_2	t_3	t_4	g_1	g_2	g_3							
	t_5	t_6	t_7	t_8	g_4	g_5	g_6							
	t_9	t_{10}	t_{11}	t_{12}	g_7	g_8	g_9							
$b=10$	t_1	t_2	t_3	t_4	g_1	g_2	g_3	t_5	t_6	t_7				
	t_8	g_4	g_5	g_6	t_9	t_{10}	t_{11}	t_{12}	g_7	g_8				
	g_9	t_{13}	t_{14}	t_{15}	t_{16}	g_{10}	g_{11}	g_{12}	t_{17}	t_{18}				
$b=14$	t_1	t_2	t_3	t_4	g_1	g_2	g_3	t_5	t_6	t_7	t_8	g_4	g_5	g_6
	t_9	t_{10}	t_{11}	t_{12}	g_7	g_8	g_9	t_{13}	t_{14}	t_{15}	t_{16}	g_{10}	g_{11}	g_{12}
	t_{17}	t_{18}	t_{19}	t_{20}	g_{13}	g_{14}	g_{15}	t_{21}	t_{22}	t_{23}	t_{24}	g_{16}	g_{17}	g_{18}

[14] Z. Jing, H. Zhiping, S. Shaojing, and Y. Shaowu, "Blind recognition of binary cyclic codes," *EURASIP J. Wirel. Commun. Netw.*, vol. 2013, no. 218, pp. 1–17, 2013.

[15] A. D. Yardi, S. Vijyakumaran, and A. Kumar, "Blind reconstruction of binary cyclic codes," *in Proc. IEEE European Wireless Conference*, 2014, pp. 1–6.

[16] M. Cluzeau and M. Finiasz, "Reconstruction of punctured convolutional codes," *in Proc. IEEE ISIT*, 2009, pp. 75–79

[17] M. Marazin, R. Gautier, and G. Burel, "Algebraic method for blind recovery of punctured convolutional encoders from an erroneous bit stream," *IET Signal Process.*, vol. 6, no. 2, pp. 122–131, April 2012.

[18] Y. Zrelli, M. Marazin, R. Gautier, E. Rannou, and E. Radoi, "Blind identification of code word length for non-binary error-correcting codes in noisy transmission," *EURASIP J. Wirel. Commun. Netw.*, vol. 2015, no. 43, pp. 1–16, 2015.

[19] T. Xia and H.-C. Wu, "Novel blind identification of LDPC codes using average LLR of syndrome a posteriori probability," *IEEE Trans. Signal Process.*, vol. 62, no. 3, pp. 632–640, Feb. 2014.

[20] R. Moosavi and E. G. Larsson, "Fast blind recognition of channel codes," *IEEE Trans. Commun.*, vol. 62, no. 5, pp. 1393–1405, May 2014

[21] P. Yu, H. Peng, and J. Li, "On blind recognition of channel codes within a candidate set," *IEEE Commun. Lett.*, vol. 20, no. 4, pp. 736–739, April 2016.

[22] Y. G. Debessu, H.-C. Wu, and H. Jiang, "Novel Blind Encoder Parameter Estimation for Turbo Codes," *IEEE Commun. Lett.*, vol. 16, no. 12, pp. 1917–1920, Dec. 2012.

[23] P. Yu, J. Li, and H. Peng, "A least square method for parameter estimation of RSC sub-codes of turbo codes," *IEEE Commun. Lett.*, vol. 18, no. 4, pp. 644–647, Apr. 2014.

[24] G. Sicot and S. Houcke, "Blind detection of interleaver parameters," *in Proc. IEEE ICASSP*, 2005, pp. 829–832.

[25] G. Golub and C. V. Loan, "Matrix computations," 3rd ed. Baltimore, MD, USA: The Johns Hopkins University Press, 1996.

[26] L. Lu, K. H. Li, and Y. L. Guan, "Blind detection of interleaver parameters for non-binary coded data streams," *in Proc. IEEE ICC*, 2009, pp. 1–4.

[27] Y-Q. Jia, L-P. Li, Y-Z. Li, and L. Gan,s "Blind estimation of convolutional interleaver parameters," *in Proc. IEEE WiCOM*, 2012, pp. 1–4.

[28] L. Gan, D. Li, Z. Liu, and L. Li, "A low complexity algorithm of blind estimation of convolutional interleaver parameters," *Science China Information Sciences*, vol. 56, no. 4, pp. 1–9, April 2013.

[29] J. F. Ziegler, "Automatic Recognition and Classification of Forward Error Correcting Codes," M.S. thesis, Dept. Elect. Comput. Eng., George Mason Univ., Fairfax, VA, USA, 2000.

[30] S. Lin and D. J. Costello, "Error Control Coding," 2nd ed. Upper Saddle River, NJ, USA: Pearson Education inc., 2004.

[31] TS 102 831 V1.2.1 (2012-08). *Digital Video Broadcasting (DVB); Implementation guidelines for a second generation digital terrestrial television broadcasting system (DVB-T2)*, Technical Specification ETSI, 2012.